The GOES I–M Imagers: New Tools for Studying Microphysical Properties of Boundary Layer Stratiform Clouds

Thomas J. Greenwald* and Sundar A. Christopher+

ABSTRACT

This study reviews the capability of the advanced imagers on Geostationary Operational Environmental Satellites (GOES) I–M to provide quantitative information about bulk microphysical properties of low-level stratiform clouds, namely, cloud liquid water path (LWP) and droplet effective radius (r_e). Previous studies show that accurate estimates of cloud LWP from GOES imagers are possible, as evaluated from both ground-based and spaceborne passive microwave measurements, provided care is taken in vicarious calibration of the visible channel. GOES estimates of r_e have yet to be validated. However, the r_e versus LWP relationship derived from GOES and Special Sensor Microwave/Imager data shows good agreement with theory. The unique high-temporal sampling of the imager allows for detailed study of daytime characteristics of cloud microphysical properties and, possibly, indirect aerosol effect. Microphysical information for drizzling marine stratocumuli was also obtained, which was confirmed by direct comparison to ship-based C-band radar during the 1997 Tropical Eastern Pacific Process Study. From the promising results obtained thus far, GOES I–M imager data should be of great value in future field experiments involving low-level stratiform clouds.

I. Introduction

Launch of the *Geostationary Operational Environmental Satellite-8 (GOES-8)* in April 1994 ushered in a new generation of advanced imaging and sounding instruments that promised to deliver improved spatial resolution at infrared (IR) wavelengths, better noise characteristics, and more frequent imagery (Menzel and Purdom 1994). These instruments have indeed lived up to these promises, providing data superior to their predecessors (Ellrod et al. 1998). *GOES-9* (J) and *GOES-10* (K) have since been launched, although *GOES-9* experienced problems in 1998 and had been in storage until recently.

The new imager data have been quantitatively used mainly for deriving cloud drift winds (Hasler et al. 1998) and land and sea surface temperature (Legeckis and Zhu 1997; Wu et al. 1999; Faysash and Smith 1999) and detecting fires (e.g., Prins et al. 1998). Unfortunately, many atmospheric scientists are unaware that these measurements may also be used to derive cloud microphysical properties. This is understandable given that these data were not meant for this purpose and that the majority of users of GOES imagery use the data in operational weather forecasting. Several recent studies, however, have presented strong evidence that useful quantitative estimates of cloud liquid water path (LWP) and cloud droplet size can be obtained. Greenwald et al. (1997) derived the first estimates of these quantities for marine stratocumulus systems using the *GOES-8* imager. Other studies have used imager data to derive physical properties from stratocumulus (Turk et al. 1998; Greenwald et al. 1999; Greenwald and Christopher 1999) and ice clouds (Young et al. 1998).

Our motivation for this paper is to raise awareness in the atmospheric science community of the capability of the GOES I–M imagers for observing microphysical properties of low-level stratiform water

*Cooperative Institute for Research in the Atmosphere, Colorado State University, Fort Collins, Colorado.
+Department of Atmospheric Sciences, University of Alabama, Huntsville, Alabama.
Corresponding author address: Dr. Thomas J. Greenwald, Cooperative Institute for Research in the Atmosphere, Colorado State University, Foothills Campus, Fort Collins, CO 80523-1375.
E-mail: greenwald@cira.colostate.edu
In final form 24 March 2000.

clouds. We present an overview of these capabilities by summarizing the results of several recently published studies. In the next section we outline the physical principles behind the retrieval of cloud droplet size and optical depth from visible and near-IR reflectance data. Instrument calibration is discussed in the following section. Next, a summary of recent efforts to test the GOES retrievals is given. This is followed by two sections on different applications of the imager, with the latter being a new application for drizzling stratocumulus systems. We summarize in the final section.

2. Theory and application

To understand how cloud physical properties are obtained from visible/near-IR satellite measurements we must first discuss basic physical concepts. Ignoring for the moment aerosols and atmospheric gases, a satellite visible sensor measures sunlight scattered by clouds and reflected by the surface. Because cloud droplets scatter sunlight efficiently (i.e., they absorb a negligible amount of light) we can show that the reflectance of a single-layer, vertically uniform cloud is largely dependent on its opacity (or optical depth). This fact has been the basis of cloud optical depth products produced by the International Satellite Cloud Climatology Project (ISCCP) since 1983 (Rossow and Schiffer 1991).

When inferring optical depth from visible reflectance we assume clouds have physical properties that vary only vertically (i.e., they are plane-parallel). This approximation allows the radiative transfer equation to be solved somewhat more easily and with less computational effort. When considering measured reflectances of real clouds, however, broken cloudiness and horizontal variations in cloud microphysical properties make interpretation more difficult. A reason we limit ourselves here to stratus and stratocumulus is that these cloud types are relatively stratified (as their names imply) and have large horizontal extent in comparison to the instrument's spatial resolution. Therefore, we can feel at least somewhat confident in applying our plane-parallel radiative transfer models. But even for these cloud types Loeb and Coakley (1998) show that the plane-parallel assumption causes biases in retrievals of cloud optical depth (up to 30%) for certain solar and viewing geometry. Using 3D Monte Carlo simulations, O'Hirok and Gautier (1998) found that errors in remotely sensing cloud optical depth using plane-parallel theory result mainly from the nonlinear relationship between reflectance and optical depth. When remotely sensing cloud particle size the major source of errors were attributed to 3D effects that instead enhance cloud droplet absorption.

At slightly longer wavelengths in the near-IR (1–4 μm) cloud water droplets become less efficient at scattering sunlight because they absorb more inci-

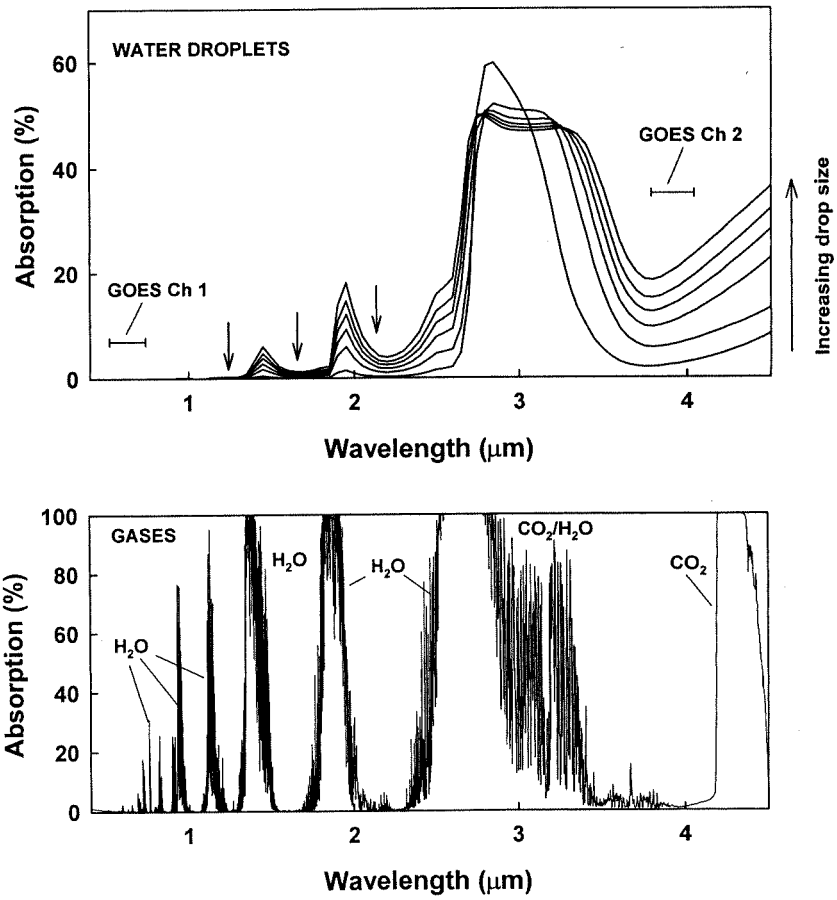

FIG. 1. (top) Absorption by different distributions of spherical water droplets vs wavelength. Each distribution has a different mean drop size. Also indicated are the commonly measured spectral regions (down-pointing arrows) and those regions measured by GOES imager channels 1 and 2. (bottom) Absorption by gases as a function of wavelength for a midlatitude summer atmosphere.

dent light. You see this in Fig. 1, which depicts absorption versus wavelength for droplet size distributions with different characteristic sizes (for now let us assume this characteristic size is roughly the mean radius of the distribution). These calculations used a modified gamma distribution (Deirmendjian 1969):

$$n(r) = \mathrm{a}r^{\alpha} \exp(-br^{\gamma}),$$

where (1)

$$b = \frac{\alpha}{\gamma r_m^{\gamma}}$$

and r is the droplet radius, r_m is the droplet mode radius, a is related to the total number of droplets per unit volume, γ is a constant, and α (an integer) defines the width of the distribution.

Generally speaking, larger droplets absorb more than smaller droplets at near-IR wavelengths. This means that measuring solar reflectance at select wavelengths allows you to infer mean particle size. Because strong molecular absorption bands (principally H_2O and CO_2) also occur at these wavelengths, channels are selected in window regions at 1.25, 1.65, and 2.15 μm and from 3.7 to 3.9 μm (see Fig. 1). Sagan and Pollack (1967) were the first to apply this idea to measurements of Venusian clouds to deduce particle size. This method has since been applied to many different instruments on both satellite and aircraft platforms (e.g., Nakajima et al. 1991; Han et al. 1994; Greenwald et al. 1999).

Now that we have a method for estimating a characteristic size of a distribution of water droplets, what characteristic size best represents the distribution with respect to its optical properties? One quantity often used in remote sensing is effective radius (r_e), which is the ratio of the third moment of the size distribution to its second moment (or the ratio of volume to cross-sectional area):

$$r_e = \frac{\int_0^{\infty} r^3 n(r) dr}{\int_0^{\infty} r^2 n(r) dr}. \quad (2)$$

Choosing r_e makes physical sense because the scattering of sunlight depends on the cross-sectional area of the particles. Also, the optical properties of the distribution mostly depend on r_e and less on the details of the distribution (e.g., Hu and Stamnes 1993). We will discuss later the effect of changes in the width of the distribution on retrieving r_e. Another advantage is that r_e can be related directly to LWP [or vertically integrated liquid water content (LWC)] by combining (2) and definition of τ as (Stephens 1978)

$$\mathrm{LWP} \approx \frac{4\tau r_e \rho_w}{3Q_{\mathrm{ext}}},$$

where ρ_w is liquid water density and Q_{ext} is extinction efficiency (≈ 2 at visible wavelengths). This expression assumes r_e is constant with height. When r_e increases with height this overestimates LWP. But since optical depth primarily determines LWP, errors incurred by this assumption are generally small.

Thermal emission from clouds also contributes significantly to the radiance measured by a near-IR sensor. This component of the measured radiance must be removed. There are different ways of accomplishing this. The most common approach is to assume cloud transmittance is negligible and that the cloud scatters radiation isotropically (i.e., equally in all directions). Based on these assumptions, we can derive a simple relationship for the reflection function (Allen et al. 1990):

$$R = \frac{I_m - B(T)}{\pi \mu_o F_o - B(T)}, \quad (3)$$

where I_m is measured radiance, B is the Planck function at temperature T, F_o is incident solar flux, and μ_o is the cosine of the solar zenith angle. A window channel measurement (e.g., 11 μm) is often used to approximate T. Miller (2000) has shown using GOES data during a total solar eclipse that (3) holds for optically thicker clouds, but breaks down for thin clouds. We also expect (3) to fail for low sun angles where scattered sunlight is nonisotropic.

In practice, one must first identify low-level stratiform water clouds before applying the retrieval method. For analyzing a few cases, identification is simply done by visually inspecting satellite imagery. However, there exist objective ways of detecting and tracking low-level stratiform clouds based on near-IR and IR window measurements (e.g., Lee et al. 1997). Once a scene has been identified, a combination of solar reflectance measurements from one visible channel and one near-IR channel are used to simultaneously estimate τ and r_e. We do this simultaneously because

there is also a slight dependence of the visible reflectance on r_e[1] and near-IR reflectance also depends on τ for optically thin clouds.

The most common approach for retrieving τ and r_e is the use of precomputed tables (e.g., Nakajima and King 1990; Platnick and Valero 1995; Greenwald et al. 1999). These tables are generated by first assuming a functional form of the droplet size distribution and calculating the optical (i.e., single scatter) properties using Lorenz–Mie theory. Then a plane-parallel radiative transfer model (which includes multiple scattering) is used to compute cloud visible and near-IR reflectance for different τ, r_e, viewing angle, and solar geometry. In these calculations we also assume a surface reflectance depending on surface type. The reflectance of ocean surfaces at these wavelengths is fairly well known. Because it is small (for an overhead sun about 6% in the visible and 2.5% in the near-IR) and has minimal variability, ocean surface reflectance has little impact on cloud property retrievals. Reflectance of land surfaces is larger and has greater variability, but only affects retrievals for optically thinner clouds (Platnick and Valero 1995). Snow and ice surfaces, however, pose the greatest challenge where specific methods have been developed for these conditions (see, e.g., Han et al. 1999).

[1]This dependence is caused by smaller particles scattering back more sunlight relative to larger particles, not because of particle absorption.

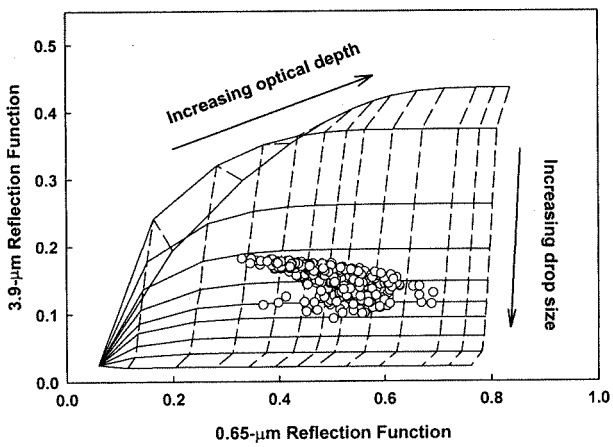

FIG. 2. Retrieval grid for *GOES-8* imager channels 1 (0.65 μm) and 2 (3.9 μm) reflectances depicting lines of constant optical depth (dashed curves) and droplet effective radius (solid curves). Calculations were made over an ocean surface for zenith angle of 58°, solar zenith angle of 29°, and relative azimuth angle of 67°. Also shown are sample measurements.

An example table (or retrieval grid) is given in Fig. 2 for *GOES-8* imager channels. The grid is plotted in reflectance space showing lines of constant τ and r_e. Because the grid resolution is finite, unique values for these quantities are obtained through interpolation. Nonuniqueness in the retrieval solution can occur for optically thin clouds made of small droplets (see "folding over" of grid in left portion of Fig. 2). This happens because as particle size decreases water droplets lose their scattering efficiency faster at longer wavelengths (Nakajima and King 1990).

For reasons of simplifying the discussion we have excluded many other aspects of the retrievals (such as accounting for gaseous absorption and the fact that clouds do not emit as blackbodies at near-IR wavelengths). Platnick and Valero (1995) provide a thorough discussion of the retrieval process. For an extended review of the theory and limitations you may refer to the excellent paper by Nakajima and King (1990).

An important issue that needs further discussion is the effect of the assumed droplet size distribution on r_e retrievals. Without independent information regarding the cloud microphysics we must make assumptions concerning the form of the size distribution in order to constrain the retrieval problem. This introduces some uncertainty because size distributions of the same or slightly different functional form that vary in width can yield slightly different cloud optical properties. Wetzel and Vonder Haar (1991) found that by changing the effective variance (v_e) of a modified gamma distribution from 0.1 to 0.3 you could alter r_e retrievals by 2–3 μm. Platnick and Valero (1995) used $v_e = 0.1 \pm 0.05$ for a gamma distribution and found errors of 10%–15% for r_e of 10–20 μm. They also found that using a normal distribution with the same v_e as the gamma distribution produced positive biases of 0.2–0.5 μm. Based on an examination of available in situ measurements, Miles et al. (2000) concluded that the width of the size distribution for stratus is highly variable and thus will have important implications for remote sensing.

A valid question to ask is what does the retrieved value of r_e really represent? Nakajima and King (1990) explained that for longer near-IR wavelengths (2.15 μm and higher) it is the effective radius of droplets somewhere near cloud top. More precisely, its magnitude is about 85%–95% (depending on cloud's opacity, vertical variation of r_e, etc.) of the magnitude of r_e at cloud top. This interpretation changes, however, for shorter near-IR wavelengths (e.g., 1.25 μm) be-

cause of a somewhat greater degree of multiple scattering that enables photons to reach deeper inside a cloud. This difference can be exploited to provide a crude vertical profile of r_e by measuring reflectance at several different near-IR wavelengths (e.g., Nakajima and Nakajima 1995; Chang et al. 1999).

3. Calibration issues

Deriving useful quantitative information from satellite sensor measurements demands accurate calibration. All channels of the GOES imagers undergo extensive calibration prior to launch (Weinreb et al. 1997). Only the infrared channels (2–5) have onboard calibration, which consists of viewing space (every 2–37 s) and a warm blackbody source (every 30 min). These procedures ensure a measurement accuracy of 1 K or better (Ellrod et al. 1998). Johnson and Weinreb (1998) recently found unexpected calibration errors of up to 1 K occurring at midnight, particularly for channels 2 and 3. They believe these errors occur during the onboard calibration process and are not caused by changes in the instrument itself. Weinreb et al. (1997) provide a detailed discussion of operational calibration procedures. For reference, we show characteristics of the imager channels in Table 1.

The visible channel on the GOES imager is more problematic because it was intended to supply only qualitative imagery. Because calibration errors are one of the largest sources of uncertainty in retrieving visible optical depth from satellite radiance measurements (Pincus et al. 1995) a lack of onboard calibration makes reliable retrievals difficult. This drawback, however, should not preclude the use of GOES visible channel measurements in studies of cloud physical properties.

There have been several recent attempts to assess and monitor the visible channel calibration through vicarious means (e.g., Bremer et al. 1998; Rao et al. 1999; Nguyen et al. 1999). These studies all report that both *GOES-8* and *-9* imagers have undergone signal degradation, which may be caused by the accumulation of material on the scanning mirror (Ellrod et al. 1998). The *GOES-8* imager visible channel also suffered an unexplained drop of about 9% in signal response soon after launch (Ellrod et al. 1998). Based on GOES imager measurements of clear ocean scenes, Knapp and Vonder Haar (2000) has estimated this initial drop in response to be about 10%. The subsequent rate of degradation for the *GOES-8* imager visible channel has been estimated to be about 7.6% per year based on measurements of starlight (Bremer et al. 1998). These results are consistent with a simple *GOES-8–9* intercalibration test used by Greenwald et al. (1997). On the other hand, Rao et al. (1999) have shown a slightly more modest decrease of about 5% per year and Knapp and Vonder Haar (2000) obtained a similar rate of degradation of 5.6%. As of November 1999 the *GOES-8* degradation is estimated to be about 40% using the results of Bremer et al. (1998). This is large enough to have a significant impact on cloud and aerosol optical depth estimates. The current best estimate of degradation rate for the *GOES-9* visible channel is about 4.9% per year (Bremer et al. 1998).

Clearly, additional work needs to be done to provide more precise calibration of the visible channel on the GOES imagers. These efforts are on going. Preliminary work suggests the absolute calibration of

TABLE 1. Characteristics of the GOES I–M imagers.

Channel	Wavelength range (μm)	Effective spatial resolution (km × km)	Precision specs (*% albedo or K at 300 K)	Description
1	0.52–0.74	0.57 × 1	0.20*	Visible
2	3.79–4.04	2.3 × 4	0.23	Near-infrared
3	6.47–7.06	4 × 8	0.22	IR water vapor
4	10.2–11.2	2.3 × 4	0.14	IR window
5	11.6–12.5	2.3 × 4	0.26	IR window/water vapor

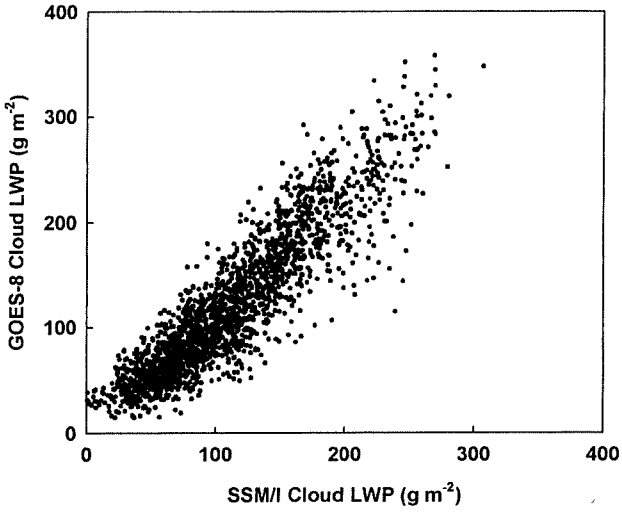

FIG. 3. Comparison between cloud LWP derived from the *GOES-8* imager and the spaceborne Special Sensor Microwave/Imager for overcast marine stratocumulus conditions (from Greenwald et al. 1997).

the visible channels should be achievable to within 10% and possibly 5%. Limited, detailed comparisons between GOES cloud LWP retrievals and surface observations appear to support this view (Greenwald et al. 1999).

4. Reliability tests of retrievals

Evaluating the quality of retrieved cloud microphysical properties is a major challenge. Two studies have looked at testing GOES cloud LWP retrievals using passive microwave radiometer observations. Microwave techniques provide a more direct estimate of LWP[2] and have a major advantage of not requiring information about the droplet size distribution. Satellite microwave techniques have also been shown to compare very well to both surface microwave radiometer (Greenwald et al. 1993) and in situ aircraft measurements (Cober et al. 1996). Furthermore, such comparisons are also important in demonstrating the consistency (or lack thereof) between these two measurement approaches that estimate the same geophysical parameter but exploit very different physical processes.

[2]LWP estimated from passive microwave measurements is directly proportional to the amount of absorption through the full depth of a cloud.

Greenwald et al. (1997) used LWP retrievals from the Special Sensor Microwave/Imager[3](SSM/I) to test *GOES-8* retrievals for a marine stratocumulus system (Fig. 3). The SSM/I was chosen in the comparison because it was, at the time, the only spaceborne-scanning microwave instrument available. They found very good agreement for closed-cell clouds (correlation of 0.91).

In another study, Greenwald et al. (1999) used high-temporal resolution (20 s) upward-looking microwave observations of cloud LWP to assess *GOES-9* retrievals (see Fig. 4). The comparisons consisted of 15-min *GOES-9* data over two Atmospheric Radiation Measurement–Cloud and Radiation Test Bed (ARM–CART) sites in Oklahoma. The results of the comparison prior to 1900 UTC yielded a high correlation (0.94). However, later in the day over the Morris, Oklahoma site large differences occurred, which were attributed to drizzle formation (Greenwald et al. 1999).

Opportunities to validate GOES retrievals of drop let effective radius have unfortunately not been avail-

[3]SSM/I is a multichannel microwave instrument that has been aboard several Defense Meteorological Satellite Program sun-synchronous satellites since 1987. Its spatial resolution ranges from about 55 km at lower frequencies to 15 km at higher frequencies.

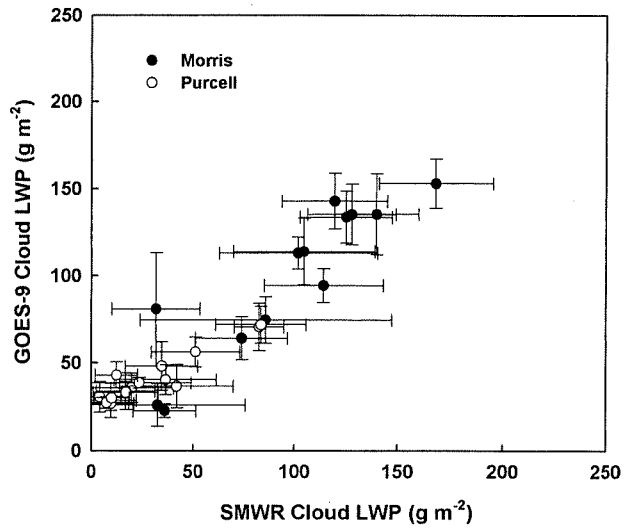

FIG. 4. Comparison between cloud LWP derived from *GOES-9* imager and upward-looking surface microwave radiometer (SMWR) observations over the Morris and Purcell, Oklahoma, ARM-CART sites on 2 May 1996 (from Greenwald et al. 1999).

able. We expect future validation efforts will likely involve in situ aircraft measurements. A limited number of these comparisons have already been conducted for Advanced Very High Resolution Radiometer[4](AVHRR) retrievals (e.g., Nakajima et al. 1991; Platnick and Valero 1995). Another possibility may be to compare the GOES estimates to those inferred from multiangle reflectance polarization measurements from the Polarization and Directionality of the Earth's Reflectance instrument (Breon and Goloub 1998).

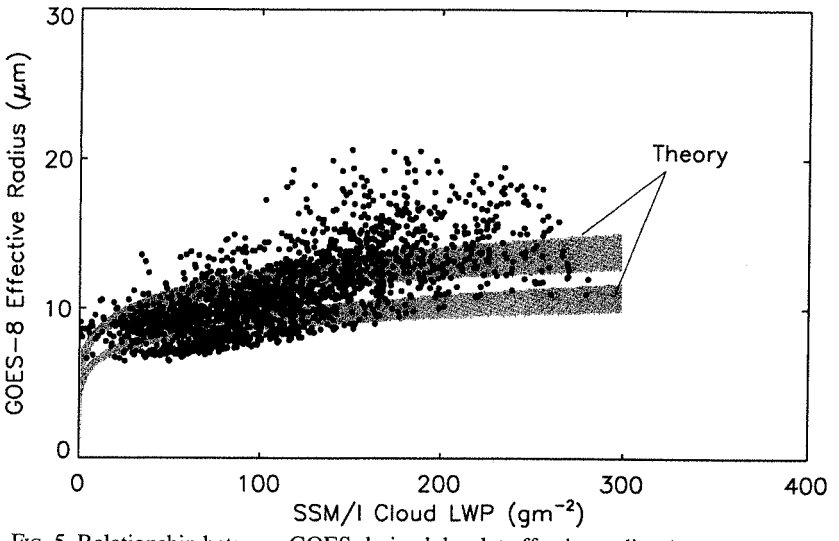

FIG. 5. Relationship between GOES-derived droplet effective radius (near cloud top) and Special Sensor Microwave/Imager–derived cloud LWP for the same case as in Fig. 3. "Theory" is the parameterization of Martin et al. (1994) assuming an effective radius invariant with height (lower shading) and varying linearly with height with a value at cloud base half that at cloud top (upper shading).

In the absence of independent verification data for the GOES effective radius retrievals we present an indirect evaluation. Greenwald et al. (1997) examined the relationship between r_e and cloud LWP using completely independent datasets from *GOES-8* and SSM/I (see Fig. 5) and found a weak positive relationship between the two. Some degree of correlation is not entirely unexpected since in situ data have indicated a weak relationship (e.g., Nakajima et al. 1991 and references therein). Also, stratocumuli are often known to nearly follow adiabatic thermodynamics since entrainment is usually small and limited to cloud top (Martin et al. 1994). The adiabatic nature of marine stratocumuli has been confirmed, for example, by Albrecht et al. (1990) using high-temporal resolution surface measurements during the First ISCCP Regional Experiment (FIRE).

For comparison to the observations, we made theoretical calculations using a physical parameterization between r_e and liquid water content (L) given by Martin et al. (1994):

$$r_e = \left[\frac{3L}{4\pi\rho_w \kappa N_{\text{tot}}}\right]^{\frac{1}{3}}, \qquad (4)$$

where N_{tot} is total droplet concentration. We chose this relationship because of its simplicity and, as shown from in situ measurements, because it predicts the droplet effective radius rather well (Martin et al. 1994). The key assumption in (4) is that the cube of the mean volume radius of the cloud drops is directly proportional to the cube of r_e through the parameter κ. In situ measurements have shown this to be a reliable approximation for stratocumulus clouds, where $\kappa = 0.80 \pm 0.07$ in marine environments (Martin et al. 1994). In these calculations we assumed a reasonable total droplet concentration of 160 cm^{-3}. We determined the geometric thickness of the clouds (needed for the LWP calculations) from the relationship between LWP and cloud thickness determined by Albrecht et al. (1990). We assumed a 30% variation in cloud thickness. The vertical variation of r_e within the cloud is unknown, so two separate ranges of curves were generated, one with a constant r_e throughout the cloud (lower shading in Fig. 5) and one in which r_e at cloud base is half the value at cloud top and varies linearly in between (upper shading in Fig. 5). Our intent here is not to provide a complete theoretical depiction of the cloud systems (which is not possible because of many unknowns and absence of in situ data), but rather to put reasonable limits on the r_e–LWP relationship expected for purely adiabatic clouds.

Remarkably, as depicted by theory these observations capture the subtle increase in r_e with increasing

[4]AVHRR is a multichannel visible/IR instrument that flies on the NOAA sun-synchronous satellites. It has channels similar to the GOES imager but higher spatial resolution (about 1 km for all channels). Sun-synchronous satellites cross the equator at the same local time. They have the disadvantage of limited temporal sampling, passing over a given area usually twice a day.

LWP for moderate to large values of LWP. While these results are not a definitive evaluation of the GOES r_e retrievals, they at least provide added confidence in their reliability. The departure of some of the observations from theory (particularly $r_e > 15$ μm) suggests the influence of nonadiabatic processes (including drizzle) or possibly macroscale cloud effects on the GOES radiances.

5. Daytime cycle of microphysical properties

The advantage of collecting measurements from a geostationary platform is that it offers a detailed look at the diurnal characteristics of cloud physical properties. Greenwald and Christopher (1999) recently used 6 days of half-hourly *GOES-9* data to investigate the daytime cycle of effective radius and LWP for a marine stratocumulus system. A summary of their findings, expressed in terms of the first harmonic Fourier amplitude and phase angle,[5] is given in Fig. 6 for a stratocumulus system off the coast of California. Amplitude is a measure of the temporal variation while phase angle, as represented here, indicates the time of the maximum in the cycle. The cloud LWP cycle was found to be a very strong feature with a peak that occurred almost always in the morning near 0930 local time. This result is consistent with limited surface measurements made during FIRE (e.g., Minnis et al. 1992) and with differences found between morning and afternoon SSM/I observations made in this region (Zuidema and Hartman 1995). Many researchers believe that the strong diurnal signature in the microphysics of these cloud systems are caused by a decoupling of the cloud layer dynamics from the subcloud layer due to solar absorption (Considine 1997). The solar heating and enhanced entrainment that results in turn makes the cloud geometrically thinner during the day, thus reducing its LWP.

Greenwald and Christopher found that the daytime behavior of the droplet effective radius was slightly different than the cloud LWP. While a morning maximum in the cycle exists, it occurs somewhat earlier than the cloud LWP. An afternoon maximum is also common but the amplitudes are generally smaller and statistically insignificant (Greenwald and Christopher 1999). The cause of the diurnal cycle of the droplet size is also probably linked to the decoupling mechanism discussed earlier; however, the effects on droplet size are subtler. Considine (1997) proposed that when a cloud layer become decoupled, changes in the vertical motion along with a decrease in the cloud-top entrainment and an activation of fewer droplets results in larger droplets near cloud top. These processes play a key role in the formation of drizzle. The increase in effective radius is small, only about 1.5 μm (Considine 1997). While Greenwald and Christopher indeed show an afternoon maximum in r_e and an afternoon–morning difference of about 1 μm, we suspect that this is not associated with the formation of drizzle since the regions where the afternoon maxima occured also had the smallest values of r_e.

An unanticipated outcome of Greenwald and Christopher's study was the possibility of GOES imager measurements detecting indirect effect of aerosols on cloud formation. Their study showed a region of very small temporal variability in r_e (which was also associated with the smallest effective radii in the re gion) extending away from the southern coast of California. They surmised that this feature was caused by the introduction of continental aerosols into the relatively cleaner maritime air. Such aerosols increase the number of cloud condensation nuclei, which produce greater numbers of smaller-sized droplets that narrow the size distribution (Hudson and Li 1995). Apparently, continental aerosols not only reduce the effective size of the droplets but also diminish the intensity of the diurnal cycle of r_e. Further work will be required, however, to confirm their preliminary findings.

6. Features of precipitating clouds

The formation of drizzle in stratocumulus systems is a somewhat common, but not well-understood, phenomenon (Austin et al. 1995). The effect of drizzle formation on stratocumulus microphysics has been observed from AVHRR measurements (e.g., Nakajima and Nakajima 1995). These effects are typically manifested as a negative correlation between droplet effective radius and optical depth. This occurs because drizzle formation tends to deplete cloud liquid water content (thus reducing optical depth) while at the same time increasing the effective radius of the droplet size

[5]Fourier series are used to describe the characteristics of periodic phenomena. The series is a sum of cosine functions of varying amplitude and phase angle with different harmonics. The first harmonic is a cosine wave in which one full cycle of the wave fits precisely within the period of interest. The amplitude wave's is half its peak-to-trough height.

distribution (e.g., Considine 1997; Rosenfeld and Lansky 1998).

Understanding the role of drizzle in stratocumulus microphysics and radiative properties is important since these clouds are ubiquitous and have a large effect on the net radiation balance (e.g., Hartmann et al. 1992). Boers et al. (1996) demonstrated using in situ data that drizzle formation in marine stratocumulus could reduce cloud albedo by as much as 18%. In contrast, a study by Pincus et al. (1997) using model analyses, in situ data, and satellite data showed that precipitation is most likely not a first-order effect in influencing stratus radiative properties.

To explore the GOES I–M imager's potential for providing bulk microphysical information about drizzling marine stratocumulus systems, we chose a case study in the eastern Pacific in conjunction with the 1997 Pan American Climate Studies Tropical Eastern Pacific Process Study (TEPPS) (Yuter and Houze 2000). Measurements from a vast array of instrumentation were taken aboard the NOAA ship, *Ronald H. Brown,* which included a highly sensitive C-band (5.37 cm) doppler radar. The mission of the TEPPS was to focus on measuring precipitating clouds along the ITCZ. However, marine stratocumuli off the coast of Baja California were also studied (Yuter et al. 2000).

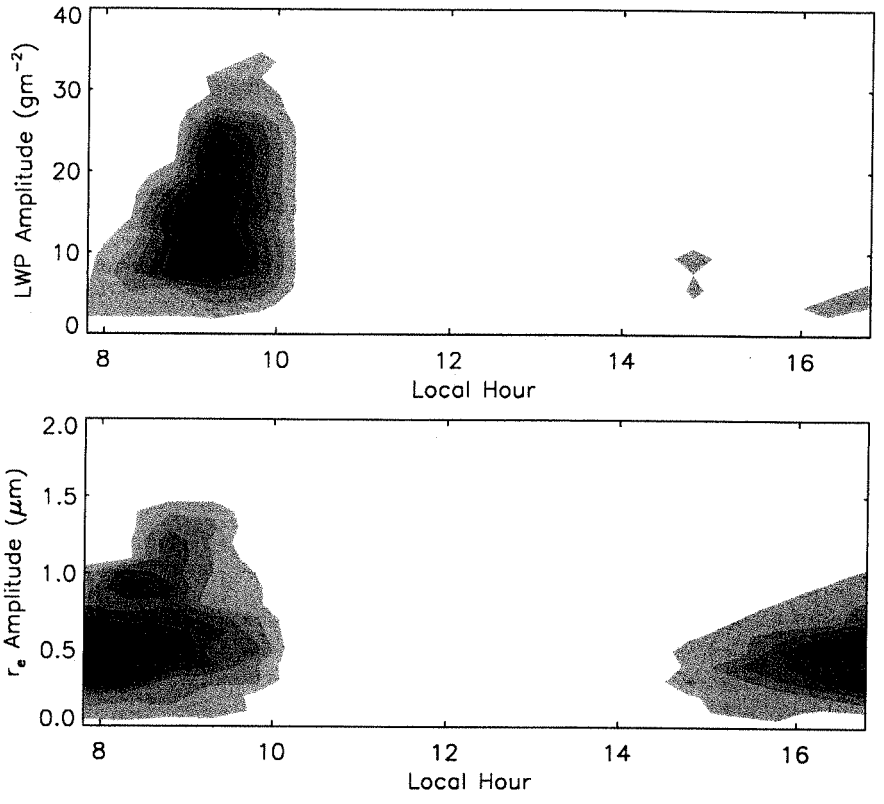

FIG. 6. (top) Frequency of occurrence for first harmonic Fourier amplitude of cloud LWP vs phase angle represented here as local time. Darker areas indicate greater occurrence. (bottom) Same as top panel except for effective radius (r_e) amplitude (Greenwald and Christopher 1999).

An excellent case was discovered at 0100 UTC 2 September 1997 that contained several lines of intense drizzle cells (see Fig. 7). Radar data at 0105 UTC indicated that the cells had reflectivities of about 5–10 dBZ with a maximum of 17 dBZ. They were also well captured in both the full-resolution visible and 3.9-μm reflectance imagery from *GOES-9.* Unlike radar, both visible and 3.9-μm channels of the imager do not actually observe the precipitation. Rather, drizzle alters the cloud microphysics, which subsequently changes the cloud radiative properties.

We can examine more closely the correspondence between these different measurements by comparing along a transect. Figure 8 shows a cross section of the radar reflectivity and GOES visible and 3.9-μm reflectances and r_e retrievals along the line A–B in Fig. 7. Note that missing r_e retrievals indicated clouds that were too optically thin for an unambiguous retrieval. Remarkably, the lowest 3.9-μm reflectance (0.05) corresponds precisely with the most intense drizzle cell. Retrievals of r_e showed that large droplet sizes (ranging from about 20 to 28 μm) were associated with these cells. In areas outside of the drizzle, r_e was 12 μm. AVHRR observations of r_e have also shown larger particle sizes for warm precipitating clouds (Rosenfeld and Gutman 1994). However, this is believed to be the first time it has been demonstrated with GOES imager data. The twin peaks in the visible reflectance also agreed well with the positions of the two drizzle cells. These results clearly demonstrate that GOES imager data contain important information regarding the microphysics of drizzling marine stratocumulus systems, data that are highly complementary to radar measurements.

GOES data also allow for a detailed tracking of the lifecycle of this system. Figure 9 shows a series of

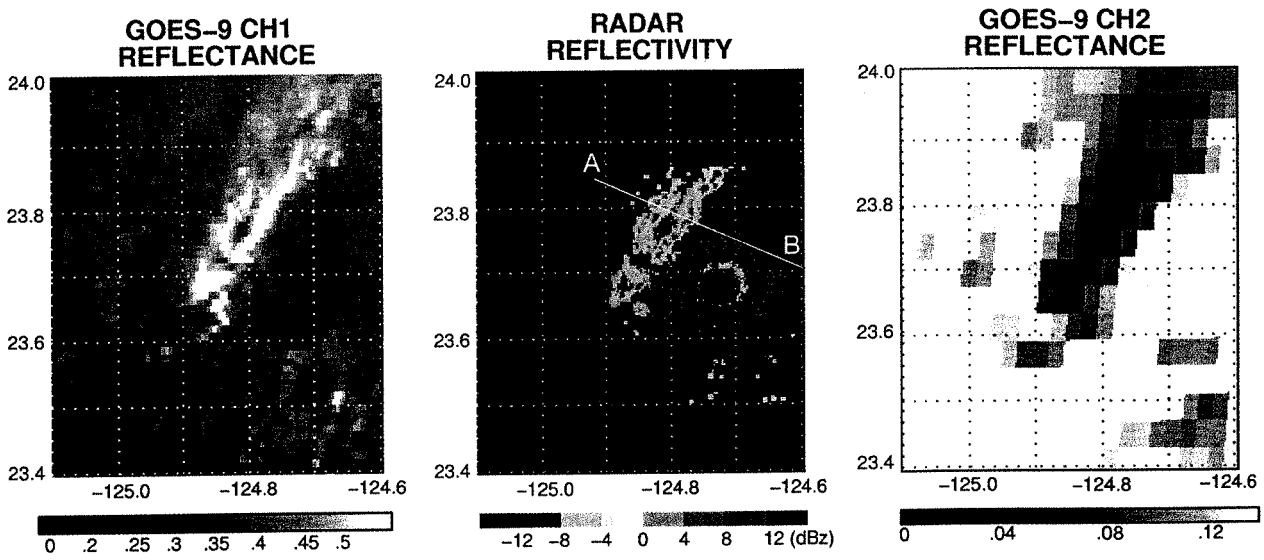

FIG. 7. Drizzle case study depicted by (left) *GOES-9* full-resolution visible imagery, (middle) C-band radar reflectivity at 1-km altitude, and (right) computed *GOES-9* channel 2 (3.9 μm) reflectance imagery.

selected *GOES-9* visible images for our case study. The system begins as a north–south line of small distinct cells that move from NE to SW. Eventually they merge to form a larger, connected series of cells that grow in size. Further insight into the formation and growth of this particular system might be gained by coupling high (space–time) resolution GOES microphysical retrievals with an analysis of the environmental conditions (e.g., Pincus et al. 1997). This is a subject of future study.

7. Summary

We have presented a review of various applications for the latest generation GOES imagers in quantitative studies of stratiform water clouds. Cloud optical depth, droplet effective radius, and liquid water path can be routinely derived from the imagers. These data (while maintaining the highest spatial–temporal resolution possible) will be crucial in evaluating cloud models that attempt to simulate the diurnal cycle of cloud microphysical properties. Currently, such datasets are not available. Generating longer-term climatic datasets in different regions should also yield greater insight into the variation of cloud microphysics. Moreover, the ability of these imagers to provide cloud microphysical information suggests they may also be useful in weather prediction through direct assimilation of radiances into numerical forecast models.

With regards to calibration, the primary concern is the visible

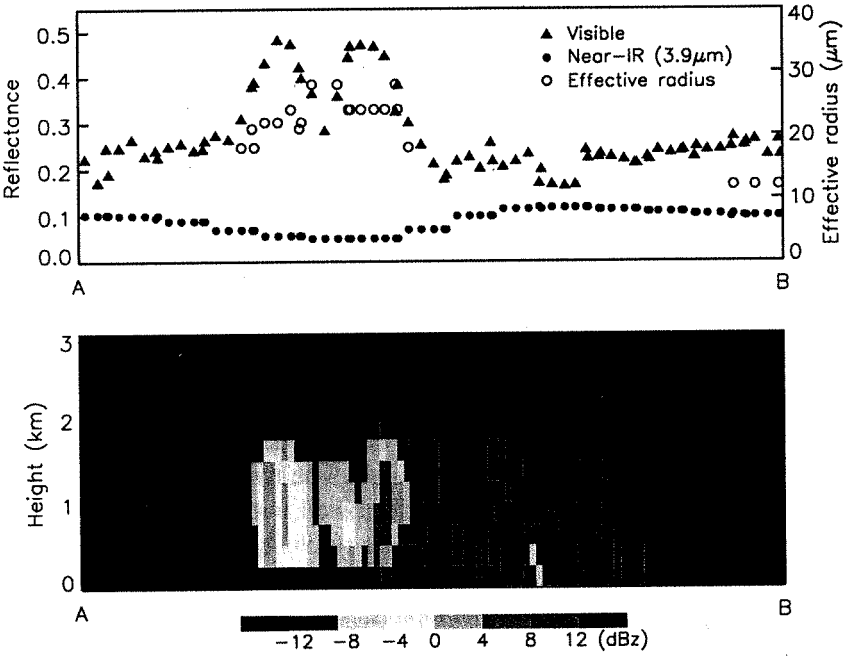

FIG. 8. (top) *GOES-9* visible reflectance, 3.9-μm reflectance, and retrievals of effective radius shown along line A–B in Fig. 7. (bottom) Corresponding cross section for C-band radar reflectivity.

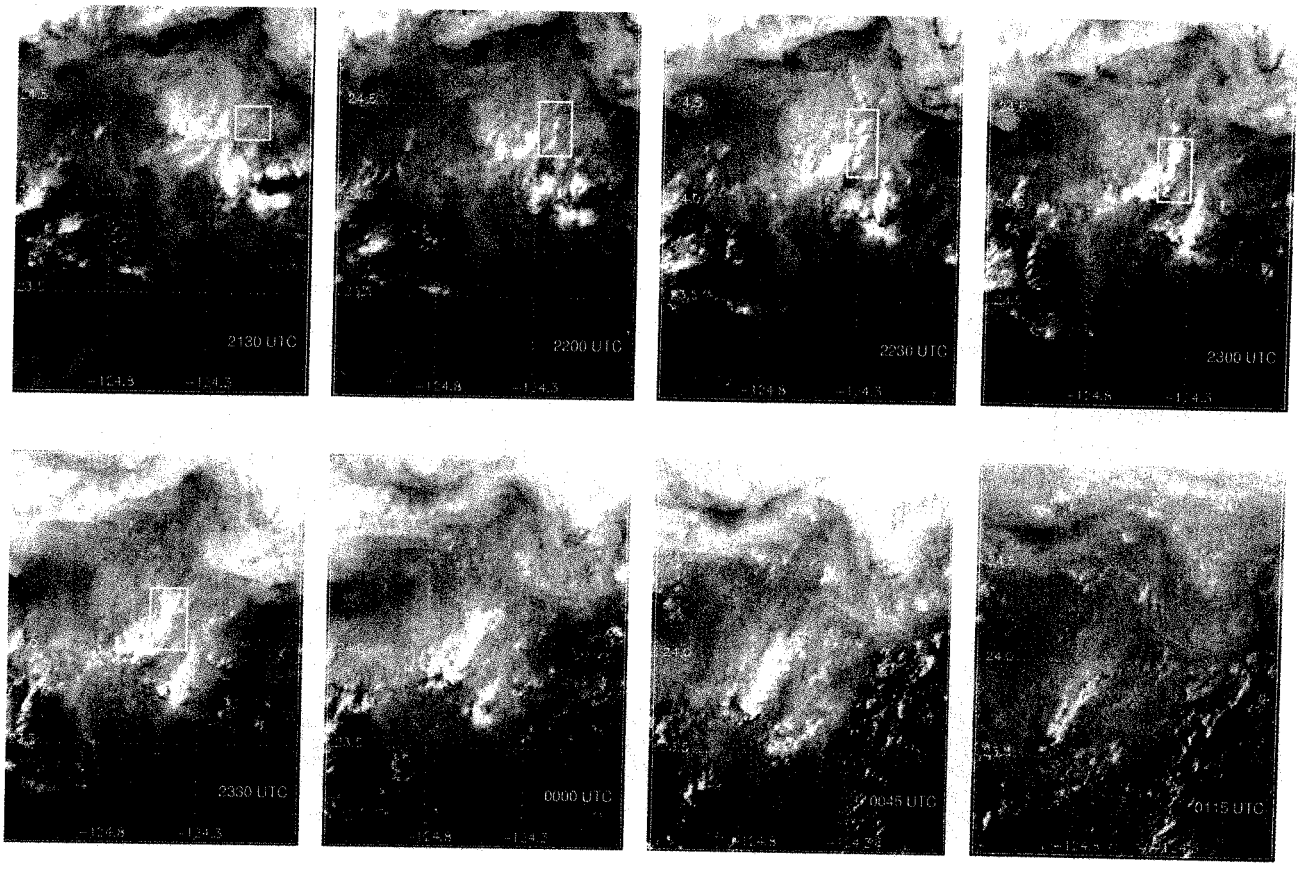

FIG. 9. *GOES-9* full-resolution visible imagery on 1 and 2 Sep 1997 illustrating the evolution of the drizzle system. White rectangles identify cells of interest.

channel. Several research groups are addressing this topic and have begun to provide estimates of the signal degradation. Available evidence based on comparisons with passive microwave satellite and surface data shows that these imagers can in fact provide accurate estimates of cloud liquid water path. The effective radius retrievals, on the other hand, have yet to be verified. Several studies also show that the assumed shape of the size distribution has an impact on these retrievals. We therefore recommend that further steps be taken to address and characterize this effect.

Indirect effect of aerosols has recently become an actively studied area of research. Rosenfeld (1999) provided the first explicit evidence from Tropical Rainfall Measurement Mission data that smoke from biomass burning suppresses rain processes in tropical clouds. The GOES imager may also detect indirect effect of aerosols and is thus likely to become one more important tool in these types of studies.

We also demonstrated that GOES I–M imager data contain quantitative information regarding the microphysics of drizzling stratocumulus clouds. Although GOES effective radius observations have somewhat coarser spatial resolution than AVHRR, these data may provide, as never before, further insight into the detailed time evolution of cloud microphysical properties and warm rain processes that sun-synchronous platforms cannot provide. On the basis of the many encouraging results from the few cloud studies that have applied GOES I–M imager data, we hope that ultimately these data will play a greater role in future experiments that seek to further understand cloud microphysical processes.

Acknowledgments. Funding was provided by the DoD Center for Geosciences Atmospheric Research Agreement DAAL01-98-2-0078. S. Christopher was supported by NASA Grant NAGW-5195. The *GOES-9* data for the drizzling stratocumulus case were obtained from the National Climatic Data Center. Thanks go to Joyce Chou for her work on the retrieval analyses and to Sandra Yuter for providing the C-band radar data.

References

Albrecht, B. A., C. W. Fairall, D. W. Thompson, A. B. White, J. B. Snider, and W. H. Schubert, 1990: Surface-based remote sens-

ing of the observed and the adiabatic liquid water content of stratocumulus clouds. *Geophys. Res. Lett.*, **17,** 89–92.

Allen, R. C., Jr., P. A. Durkee, and C. H. Wash, 1990: Snow/cloud discrimination with multispectral satellite measurements. *J. Appl. Meteor.*, **29,** 994–1004.

Austin, P., Y. Wang, R. Pincus, and V. Kujala, 1995: Precipitation in stratocumulus clouds: Observational and modeling results. *J. Atmos. Sci.*, **52,** 2329–2352.

Boers, B., J. B. Jensen, P. B. Krummel, and H. Gerber, 1996: Microphysical and shortwave radiative structure of wintertime stratocumulus clouds over the southern ocean. *Quart. J. Roy. Meteor. Soc.*, **122,** 1307–1339.

Bremer, J. C., J. G. Baucom, H. Vu, M. P. Weinreb, and N. Pinkine, 1998: Estimation of long-term throughput degradation of *GOES-8* and *-9* visible channels by statistical analysis of star measurements. *Proc. SPIE Conf. on Earth Observing Systems III,* San Diego, CA, The International Society for Optical Engineering, 145–149.

Breon, F.-M., and P. Goloub, 1998: Cloud droplet effective radius from spaceborne polarization measurements. *Geophys. Res. Lett.*, **25,** 1879–1882.

Chang, F.-L., Z. Li, and H. W. Barker, 1999: Retrieving the vertical profile of cloud droplet effective radius from multiple spectral channels. Preprints, *10th Conf. on Atmospheric Radiation,* Madison, WI, Amer. Meteor. Soc., 153–156.

Cober, S. G., A. Tremblay, and G. A. Issac, 1996: Comparisons of SSM/I liquid water paths with aircraft measurements. *J. Appl. Meteor.*, **35,** 503–519.

Considine, G. D., 1997: Modeling the diurnal variability in cloud microphysics in boundary layer clouds. *J. Geophys. Res.*, **102,** 1717–1726.

Deirmendjian, D., 1969: *Electromagnetic Scattering on Spherical Polydispersions.* Elsevier Publishing Co., 290 pp.

Ellrod, G. P., R. V. Achutuni, J. M. Daniels, E. M. Prins, J. P. Nelson III, 1998: An assessment of *GOES-8* imager data quality. *Bull. Amer. Meteor. Soc.*, **79,** 2509–2526.

Faysash, D. A., and E. A. Smith, 1999: Simultaneous land surface temperature–emissivity retrieval in the infrared split window. *J. Atmos. Oceanic Technol.*, **16,** 1673–1689.

Greenwald, T. J., and S. A. Christopher, 1999: Daytime variation of marine stratocumulus microphysical properties as observed from geostationary satellite. *Geophys. Res. Lett.*, **26,** 1723–1726.

——, G. L. Stephens, T. H. Vonder Haar, and D. L. Jackson, 1993: A physical retrieval of cloud liquid water over the global oceans using Special Sensor Microwave/Imager (SSM/I) observations. *J. Geophys. Res.*, **98,** 18 471–18 488.

——, S. A. Christopher, and J. Chou, 1997: Cloud liquid water path comparisons from solar reflectance and passive microwave satellite measurements: Assessment of sub-field-of-view cloud effects for microwave retrievals. *J. Geophys. Res.*, **102,** 19 585–19 596.

——, ——, ——, and J. C. Liljegren, 1999: Intercomparison of cloud liquid water path derived from the *GOES-9* imager and ground based microwave radiometers for continental stratocumulus. *J. Geophys. Res.*, **104,** 9251–9260.

Han, Q., W. B. Rossow, and A. A. Lacis, 1994: Near-global survey of effective droplet radii in liquid water clouds using ISCCP data. *J. Climate,* **7,** 465–497.

Han, W., K. Stamnes, and D. Lubin, 1999: Remote sensing of surface and cloud properties in the Arctic from AVHRR. *J. Appl. Meteor.*, **38,** 989–1012.

Hartmann, D. L., M. E. Ockert-Bell, and M. L. Michelsen, 1992: The effect of cloud type on earth's energy balance. *J. Climate,* **5,** 1281–1304.

Hasler, A. F., K. Palaniappan, C. Kambhammetu, P. Black, E. Uhlhorn, and D. Chesters, 1998: High-resolution wind fields within the inner core and eye of a mature tropical cyclone from GOES 1-min images. *Bull. Amer. Meteor. Soc.*, **79,** 2483–2496.

Hu, Y. X., and K. Stamnes, 1993: An accurate parameterization of the radiative properties of water clouds for use in climate models. *J. Climate,* **6,** 728–742.

Hudson, J. G., and H. Li, 1995: Microphysical contrasts in Atlantic stratus. *J. Atmos. Sci.*, **52,** 3031–3040.

Johnson, R. X., and M. Weinreb, 1998: *GOES-8* imager midnight effects and slope correction. *Proc. SPIE, GOES-8 and Beyond,* Bellingham, WA, The International Society for Optical Engineering, 596–607.

Knapp, K. R., and T. H. Vonder Haar, 2000: Calibration of the Eighth Geostationary Observational Environmental Satellite (*GOES-8*) Imager Visible Sensor. *J. Atmos. Oceanic Technol.*, in press.

Lee, T. F., F. J. Turk, and K. Richardson, 1997: Stratus and fog products using *GOES-8–9* 3.9-μm data. *Wea. Forecasting,* **12,** 664–677.

Legeckis, R., and T. Zhu, 1997: Sea surface temperatures from the *GOES-8* geostationary satellite. *Bull. Amer. Meteor. Soc.*, **78,** 1971–1983.

Loeb, N. G., and J. A. Coakley, 1998: Inference of marine stratus cloud optical depths from satellite measurements: Does 1D theory apply? *J. Climate,* **11,** 215–233.

Martin, G. M., D. W. Johnson, and A. Spice, 1994: The measurement and parameterization of effective radius of droplets in warm stratocumulus clouds. *J. Atmos. Sci.*, **51,** 1823–1842.

Menzel, W. P., and J. F. W. Purdom, 1994: Introducing *GOES-I*: The first in a new generation of geostationary operational satellites. *Bull. Amer. Meteor. Soc.*, **75,** 757–780.

Miles, N. L., J. Verlinde, and E. E. Clothiaux, 2000: Cloud droplet size distributions in low-level stratiform clouds. *J. Atmos. Sci.*, **57,** 295–311.

Miller, S. D., 2000: Physical decoupling of the GOES daytime 3.9-μm channel thermal emission and solar reflection components using total solar eclipse data. *Int. J. Remote Sens.*, in press.

Minnis, P., P. W. Heck, and D. F. Young, 1992: Stratocumulus cloud properties derived from simultaneous satellite and island-based instrumentation during FIRE. *J. Appl. Meteor.*, **31,** 317–339.

Nakajima, T., and M. D. King, 1990: Determination of the optical thickness and effective particle radius of clouds from reflected solar radiation measurements. Part I: Theory. *J. Atmos. Sci.*, **47,** 1878–1893.

——, ——, J. D. Spinhirne, and L. F. Radke, 1991: Determination of the optical thickness and effective particle radius of clouds from reflected solar radiation measurements. Part II: Marine stratocumulus observations. *J. Atmos. Sci.*, **48,** 728–849.

Nakajima, T. Y., and T. Nakajima, 1995: Wide-area determination of cloud microphysical properties from NOAA AVHRR

measurements for FIRE and ASTEX regions. *J. Atmos. Sci.,* **52,** 4043–4059.

Nguyen, L., P. Minnis, J. K. Ayers, W. L. Smith Jr., and S.-P. Ho, 1999: Intercalibration of geostationary and polar satellite imager data using AVHRR, VIRS, and ASTR-2 data. Preprints, *10th Conf. on Atmospheric Radiation,* Madison, WI, Amer. Meteor. Soc., 405–408.

O'Hirok, W., and C. Gautier, 1998: A three-dimensional radiative transfer model to investigate the solar radiation within a cloudy atmosphere. Part II: Spectral effects. *J. Atmos. Sci.,* **55,** 3065–3076.

Pincus, R., M. Szczodrak, J. Gu, and P. Austin, 1995: Uncertainty in cloud optical depth estimates made from satellite radiance measurements. *J. Climate,* **8,** 1453–1462.

——, M. A. Baker, and C. S. Bretherton, 1997: What controls stratocumulus radiative properties? Lagrangian observations of cloud evolution. *J. Atmos. Sci.,* **54,** 2215–2236.

Platnick, S., and F. P. J. Valero, 1995: A validation of a satellite cloud retrieval during ASTEX. *J. Atmos. Sci.,* **52,** 2985–3001.

Prins, E. M., J. M. Feltz, W. P. Menzel, and D. E. Ward, 1998: An overview of *GOES-8* diurnal fire and smoke results from SCAR-B and the 1995 fire season in South America. *J. Geophys. Res.,* **103,** 31 821–31 836.

Rao, C. R. N., J. Chen, and N. Zhang, 1999: Calibration of the visible channel of the GOES imager using the advanced very high resolution radiometer. Preprints, *10th Conf. on Atmospheric Radiation,* Madison, WI, Amer. Meteor. Soc., 560–563.

Rosenfeld, D., 1999: TRMM observed first direct evidence of smoke from forest fires inhibiting rainfall. *Geophys. Res. Lett.,* **26,** 3105–3108.

——, and G. Gutman, 1994: Retrieving microphysical properties near the tops of potential rain clouds by multispectral analysis of AVHRR data. *J. Atmos. Res.,* **34,** 259–283.

——, and I. M. Lensky, 1998: Spaceborne sensed insights into precipitation formation processes in continental and maritime clouds. *Bull. Amer. Meteor. Soc.,* **79,** 2457–2476.

Rossow, W. B., and R. A. Schiffer, 1991: ISCCP cloud data products. *Bull. Amer. Meteor. Soc.,* **72,** 2–20.

Sagan, C., and J. B. Pollack, 1967: Anisotropic nonconservative scattering and the clouds of Venus. *J. Geophys. Res.,* **72,** 469–477.

Stephens, G. L., 1978: Radiation profiles in extended water clouds. II: Parameterization schemes. *J. Atmos. Sci.,* **35,** 2123–2132.

Turk, J., J. Vivekanandan, T. Lee, P. Durkee, and K. Nielsen, 1998: Derivation and applications of near-infrared cloud reflectances from *GOES-8* and *GOES-9. J. Appl. Meteor.,* **37,** 819–831.

Young, D. F., P. Minnis, and D. Baumgardner, 1998: Comparison of in situ and satellite-derived cloud properties during SUCCESS. *Geophys. Res. Lett.,* **25,** 1125–1128.

Weinreb, M. P., M. Jamison, N. Fulton, Y. Chen, J. X. Johnson, J. Bremer, C. Smith, and J. Baucum, 1997: Operational calibration of Geostationary Operational Environmental Satellite-8 and -9 imagers and sounders. *Appl. Opt.,* **36,** 6895–6904.

Wetzel, M. A., and T. H. Vonder Haar, 1991: Theoretical development and sensitivity tests of a stratus cloud droplet size retrieval method for AVHRR-K/L/M. *Remote Sens. Environ.,* **36,** 105–119.

Wu, X., W. P. Menzel, and G. S. Wade, 1999: Estimation of sea surface temperatures using *GOES-8/9* radiance measurements. *Bull. Amer. Meteor. Soc.,* **80,** 1127–1138.

Yuter, S. E., and R. A. Houze Jr., 2000: The 1997 Pan American Climate Studies Tropical Eastern Pacific Process Study. Part I: ITCZ region. *Bull. Amer. Meteor. Soc.,* **81,** 451–481.

——, Y. L. Serra, and R. A. Houze Jr., 2000: The 1997 Pan American Climate Studies Tropical Eastern Pacific Process Study. Part II: Stratocumulus region. *Bull. Amer. Meteor. Soc.,* **81,** 483–490.

Zuidema, P., and D. L. Hartmann, 1995: Satellite determination of stratus cloud microphysical properties. *J. Climate,* **8,** 1638–1657.